

## *Supplementary Information*

### **Ligand-ligand interactions effect on the formation of photoluminescent gold nanoclusters embedded in Au(I)-thiolate supramolecules**

Hsiang-Yu Chang,<sup>a</sup> Yu-Ting Tseng,<sup>a</sup> Zhiqin Yuan,<sup>b</sup> Hung-Lung Chou,<sup>\*c</sup> Ching-Hsiang Chen,<sup>d</sup> Bing-Joe Hwang,<sup>d</sup> Meng-Che Tsai,<sup>d</sup> Huan-Tsung Chang<sup>\*ach</sup> and Chih-Ching Huang<sup>\*fgh</sup>

<sup>a</sup> *Department of Chemistry, National Taiwan University, Taipei 10617, Taiwan*

<sup>b</sup> *State Key Laboratory of Chemical Resource Engineering, Beijing University of Chemical Technology, Beijing 100029, China*

<sup>c</sup> *Graduate Institute of Applied Science and Technology, National Taiwan University of Science and Technology, Taipei 10617, Taiwan*

<sup>d</sup> *Nanoelectrochemistry Laboratory, Department of Chemical Engineering, National Taiwan University of Science and Technology, Taipei 10617, Taiwan*

<sup>e</sup> *Department of Chemistry, Chung Yuan Christian University, Taoyuan City 32023, Taiwan*

<sup>f</sup> *Department of Bioscience and Biotechnology, National Taiwan Ocean University, Keelung 20224, Taiwan*

<sup>g</sup> *Center of Excellence for the Oceans, National Taiwan Ocean University, Keelung 20224, Taiwan*

<sup>h</sup> *School of Pharmacy, College of Pharmacy, Kaohsiung Medical University, Kaohsiung 80708, Taiwan*

**Correspondence:** Professor Hung-Lung Chou, Graduate Institute of Applied Science and Technology, National Taiwan University of Science and Technology, 43, Section 4, Keelung Road, Taipei 10617, Taiwan. E-mail: HLCHOU@mail.ntust.edu.tw; Professor Huan-Tsung Chang, Department of Chemistry, National Taiwan University, 1, Section 4, Roosevelt Road, Taipei 10617, Taiwan. E-mail: changht@ntu.edu.tw; Professor Chih-Ching Huang, Department of Bioscience and Biotechnology, National Taiwan Ocean University, 2, Beining Road, Keelung 20224, Taiwan. E-mail: huanging@ntou.edu.tw

**Table S1** The intensities of static light scattering and zeta potentials of the products from the reactions of H<sub>2</sub>AuCl<sub>4</sub> (1.4 mM) with L-cysteine (10 mM) at pH of (A) 3, (B) 5, (C) 7, and (D) 9.

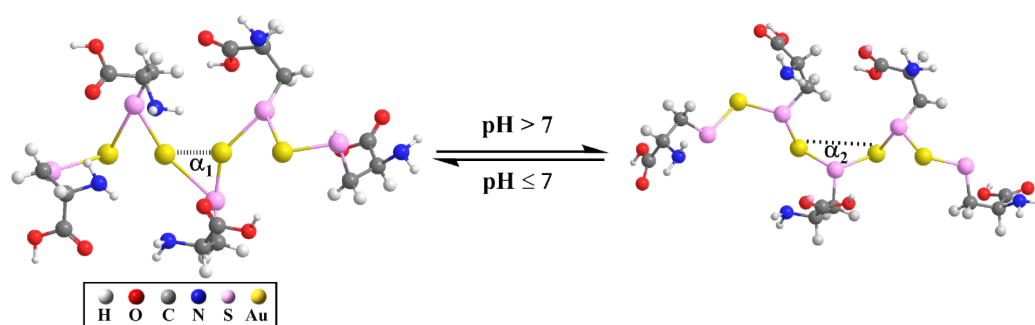
Sample	Static light scattering (kcps; n = 5)	Zeta potential (mV; n=5)
A	273.2±32.7	-0.92±4.75
B	243.2±25.6	-1.14±4.04
C	250.2±22.3	-4.53±3.70
D	74.2±18.3	-12.3±2.23

**Table S2** Optical properties of as-prepared Cys–Au NCs<sub>pH3–7</sub> and –[Cys–Au(I)]<sub>n</sub>–<sub>pH9</sub>.

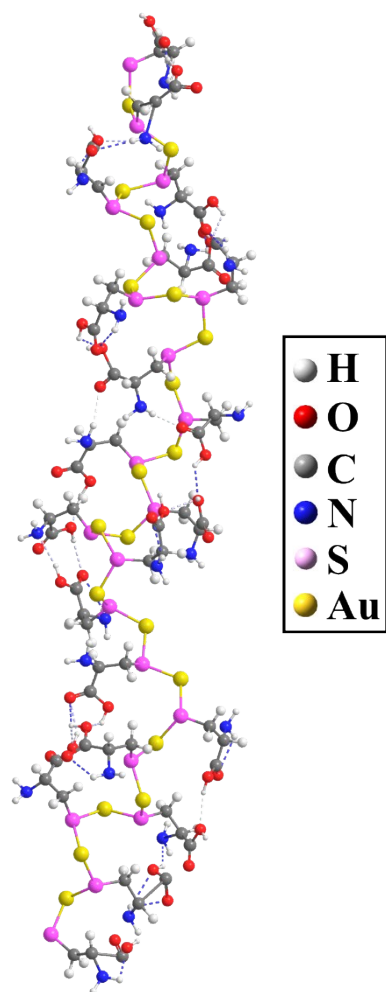
sample	$\lambda_{max}^{abs}$ (nm) <sup>a</sup>	$\lambda_{max}^{ex}$ (nm) <sup>b</sup>	$\lambda_{max}^{em}$ (nm) <sup>c</sup>	QY (%)	$\tau$ ( $\tau_1/\tau_2$ , ns)
Cys–Au NCs <sub>pH3</sub>	365	355	630	11.6	218.68 (29.05%)/2288.78 (70.95%)
Cys–Au NCs <sub>pH5</sub>	365	350	630	10.4	44.27 (39.72%)/1876.49 (60.28%)
Cys–Au NCs <sub>pH7</sub>	365	350	630	10.1	145.07 (32.59%)/2190.04 (67.41%)
–[Cys–Au(I)] <sub>n</sub> – <sub>pH9</sub>	-	-	-	0.21	42.97 (63.51%)/1196.65 (36.49%)

<sup>a</sup>absorption-band maxima at wavelength. <sup>b</sup>excitation-band maxima at wavelength.

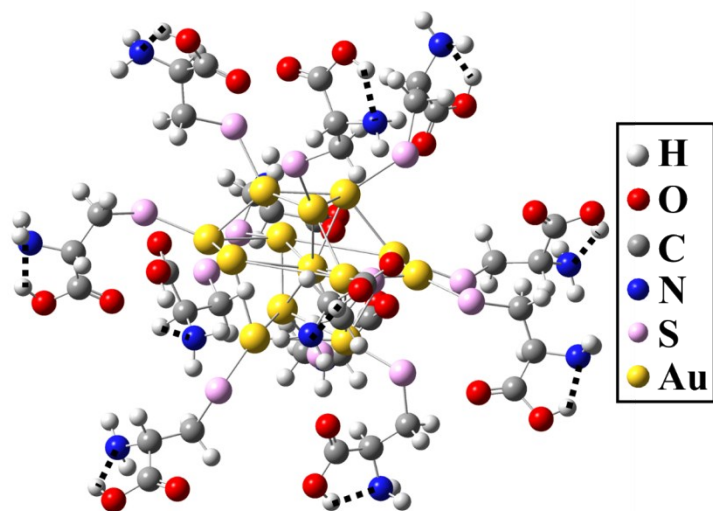
<sup>c</sup>emission-band maxima at wavelength.



**Scheme S1** Schematic of aurophilic Au(I)···Au(I) interactions mediated by the interaction between adjacent Cys ligands along the  $-\text{[Cys-Au(I)]}_n-$  polymeric backbone through controlling solution pH values. Parameters  $\alpha_1$  and  $\alpha_2$  are the Au(I)–S(R)–Au(I) angles at  $\text{pH} \leq 7$  and  $\text{pH} > 7$ , respectively.



**Scheme S2** Schematic of a helical structure of the  $-[\text{Cys-Au(I)}]_n-$  polymer.



**Scheme S3** Proposed structure of  $[\text{Au}_{13}\text{Cys}_{12}]^+$ .

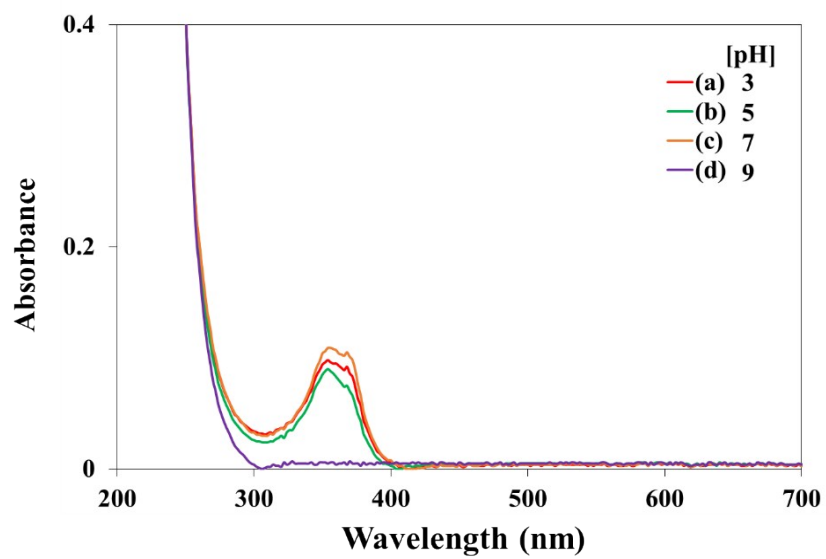


**Fig. S1** UV-Vis absorption spectra of the products from the reactions of  $\text{HAuCl}_4$  (1.4 mM) with L-cysteine (10 mM) for 1 h in solutions with pH at (a) 3, (b) 5, (c) 7, and (d) 9.

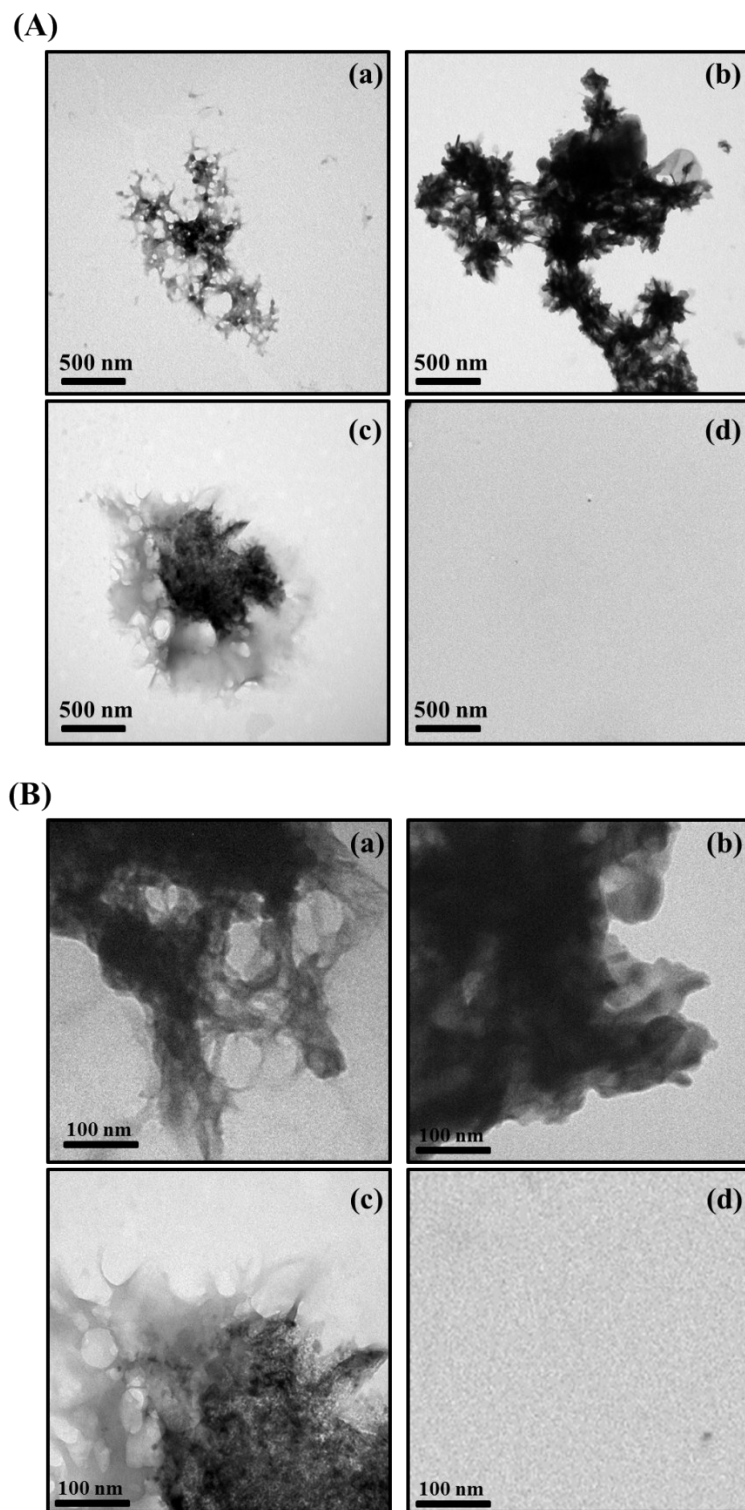


**Fig. S2** (A) Low-magnification and (B) high-magnification TEM images of the products from the reactions of  $\text{HAuCl}_4$  (1.4 mM) with L-cysteine (10 mM) for 1 h in solutions at pH (a) 3, (b) 5, (c) 7, and (d) 9.



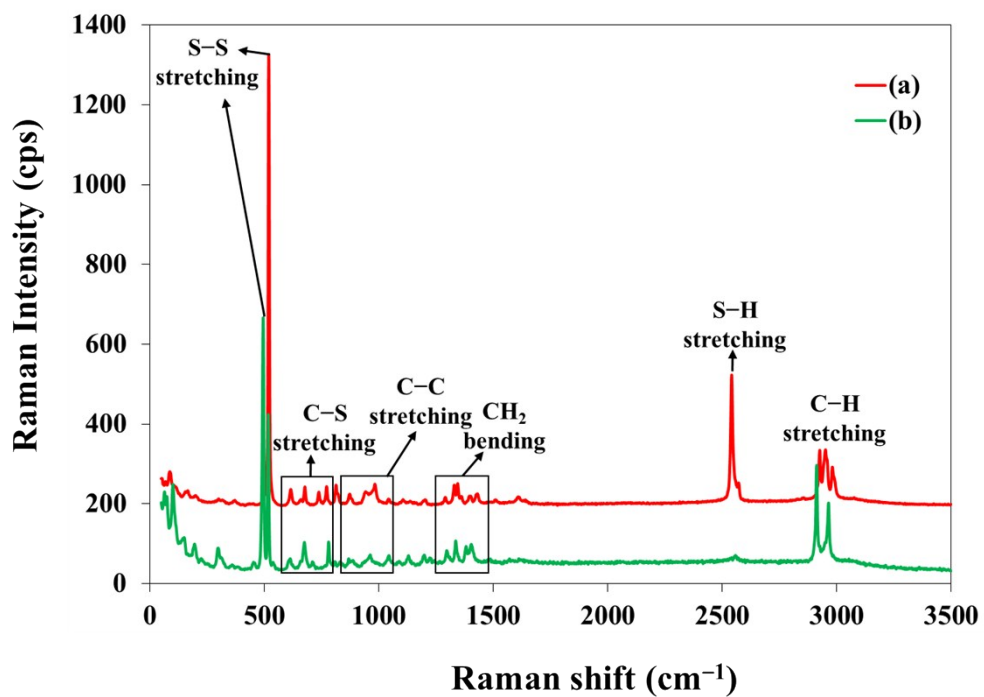


**Fig. S3** Raman spectra of (a) L-Cys and (b) as-prepared  $-\text{[Cys-Au(I)]}_n-$  supramolecules from the reaction of  $\text{HAuCl}_4$  (1.4 mM) with L-cysteine (10 mM) for 1 h in a solution at pH 3.

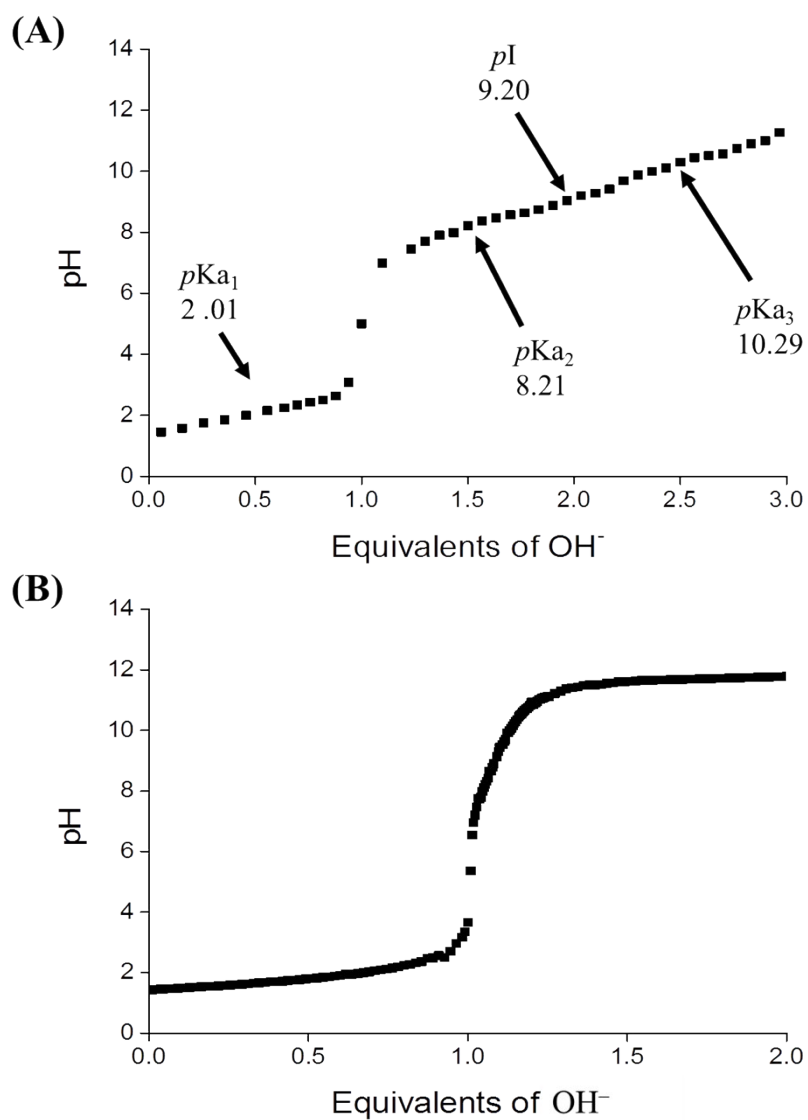


**Fig. S4** Potentiometric titration of (A) cysteine (1.4 mM) and (B) as-prepared  $-\text{[Cys-Au(I)]}_n-$  polymers/supramolecules from the reaction of  $\text{HAuCl}_4$  (1.4 mM) with L-cysteine (1.4 mM) for 1 h. The cysteine or  $-\text{[Cys-Au(I)]}_n-$  polymers/supramolecules are titrated by NaOH (100 mM).

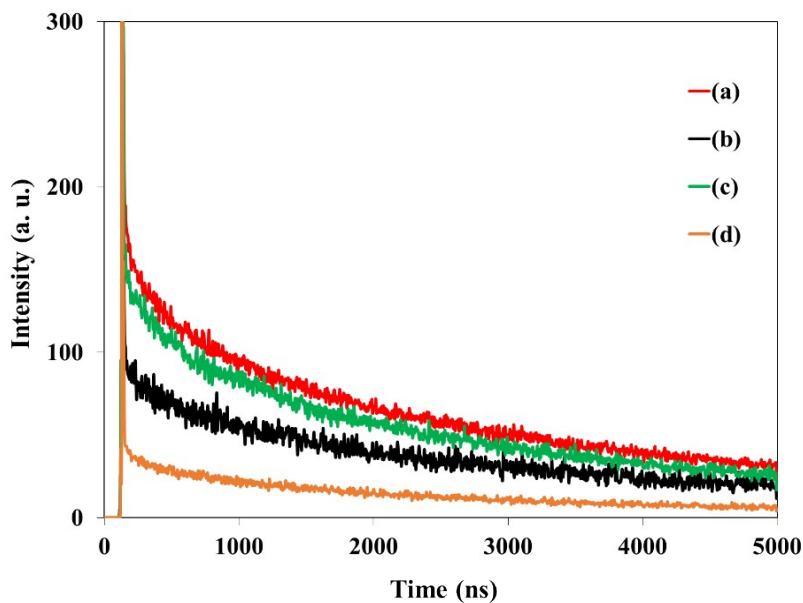


**Fig. S5** PL decays of as-prepared (a) Cys–Au NCs<sub>pH3</sub>, (b) Cys–Au NCs<sub>pH5</sub>, (c) Cys–Au NCs<sub>pH7</sub>, and (d)  $-[\text{Cys–Au(I)}]_n\text{–pH9}$  excited with a pulsed laser at 375 nm. Each of them was then fitted to a biexponential PL decay [ $I(t) = a_1\exp(-t/\tau_1) + a_2\exp(-t/\tau_2)$ ], providing lifetimes ( $\tau_1/\tau_2$ ) for the (a) Cys–Au NCs<sub>pH3</sub>, (b) Cys–Au NCs<sub>pH5</sub>, (c) Cys–Au NCs<sub>pH7</sub>, and (d)  $-[\text{Cys–Au(I)}]_n\text{–pH9}$  of 218.68 ns (29.05%)/2288.78 ns (70.95%), 44.27 ns (39.72%)/1876.49 ns (60.28%), 145.07 ns (32.59%)/2190.04 ns (67.41%), and 42.97 ns (63.51%)/1196.65 ns (36.49%), respectively.

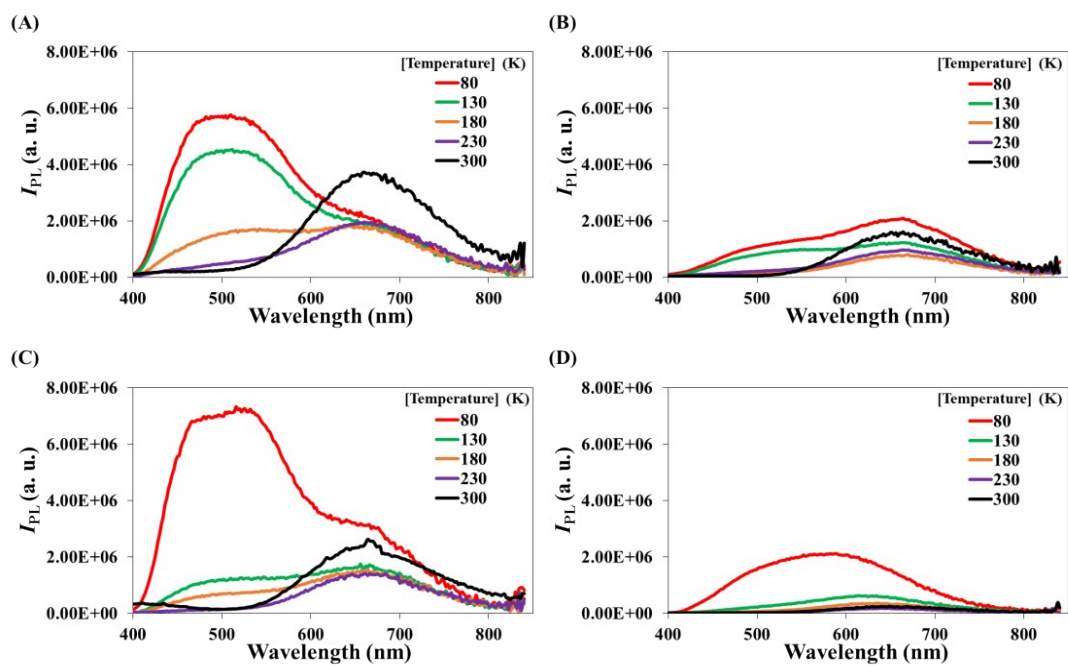


**Fig. S6** Temperature-dependent PL spectra of (A) Cys–Au NCs<sub>pH3-</sub>, (B) Cys–Au NCs<sub>pH5-</sub>, and (C) Cys–Au NCs<sub>pH7-</sub> embedded in  $-[\text{Cys–Au(I)}]_n-$  supramolecules and (D)  $-[\text{Cys–Au(I)}]_n\text{-pH9}$  at 80–300 K. The PL intensities ( $I_{\text{PL}}$ ) are plotted in arbitrary units (a. u.). Other conditions were the same as those described in Figure 2.

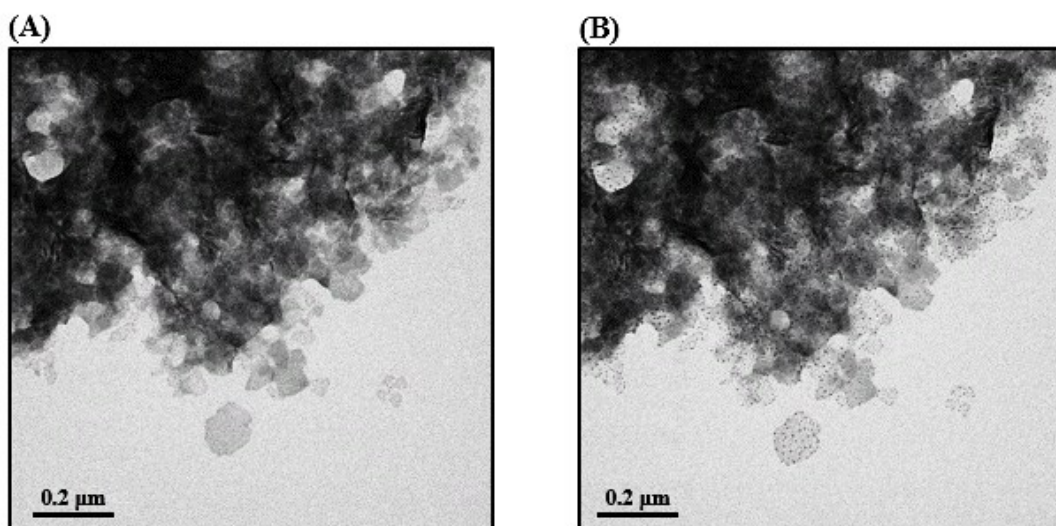


**Fig. S7**  $[\text{Cys-Au(I)}]_n^-$  supramolecules (pH 3) (A) before and (B) after continuous electron-beam irradiation (200 kV) for 10 s during TEM observation.

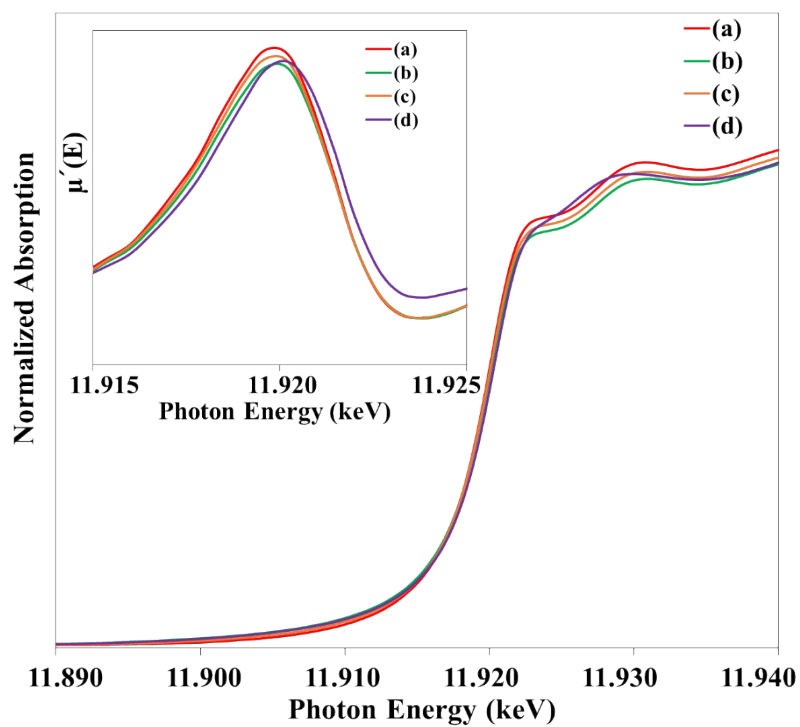


**Fig S8** XANES spectra of the Au  $L_3$ -edge of as-prepared (a) Cys–Au  $\text{NC}_{\text{pH}3^-}$ , (b) Cys–Au  $\text{NC}_{\text{pH}5^-}$ , and (c) Cys–Au  $\text{NC}_{\text{pH}7^-}$ -embedded in  $-\text{[Cys–Au(I)]}_n-$  supramolecules and (d)  $-\text{[Cys–Au(I)]}_n-\text{pH}9$ . Inset: first-derivative spectra of the corresponding samples.

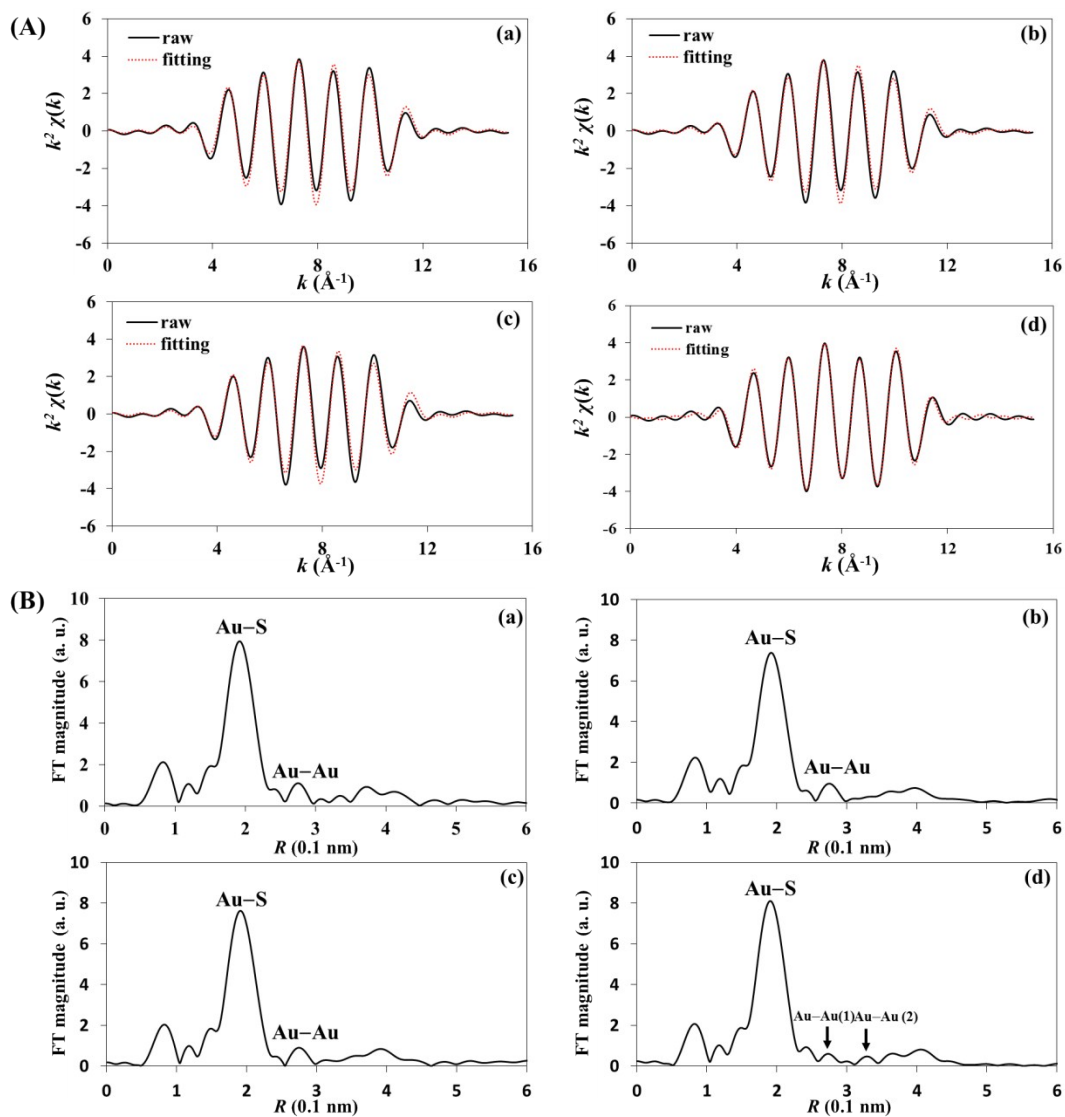


**Fig. S9** (A)  $k^2\chi(k)$  and the least-squares EXAFS curve-fitting data and (B) Fourier-transformed curves of the  $k^2\chi(k)$  functions of the as-prepared (a) Cys–Au NCs<sub>pH3<sup>-</sup></sub>, (b) Cys–Au NCs<sub>pH5<sup>-</sup></sub>, and (c) Cys–Au NCs<sub>pH7</sub>-embedded in  $-[\text{Cys–Au(I)}]_n-$  supramolecules and (d)  $-[\text{Cys–Au(I)}]_n-$ <sub>pH9</sub>.

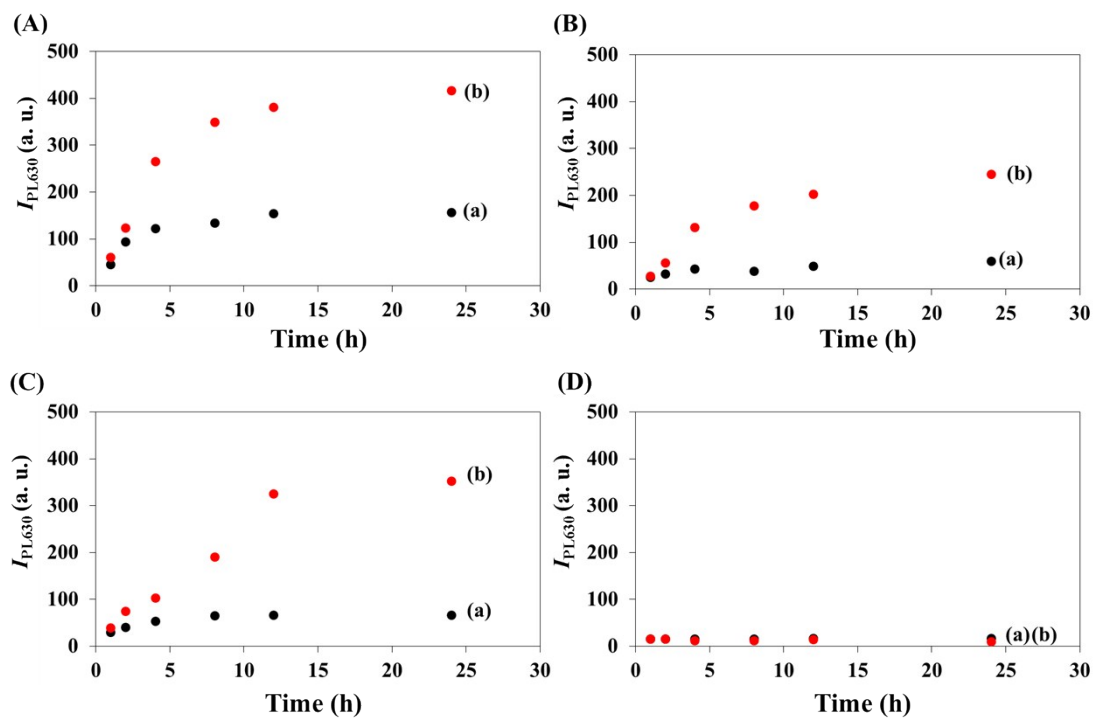


**Fig. S10** Time-course measurement of PL intensity at 630 nm ( $I_{PL630}$ ) for  $-[Cys-Au(I)]_n-$  polymers/supramolecules in solutions with pH at (A) 3, (B) 5, (C) 7, and (D) 9 in the (a) absence or (b) presence of  $NaBH_4$  (0.75 mM).



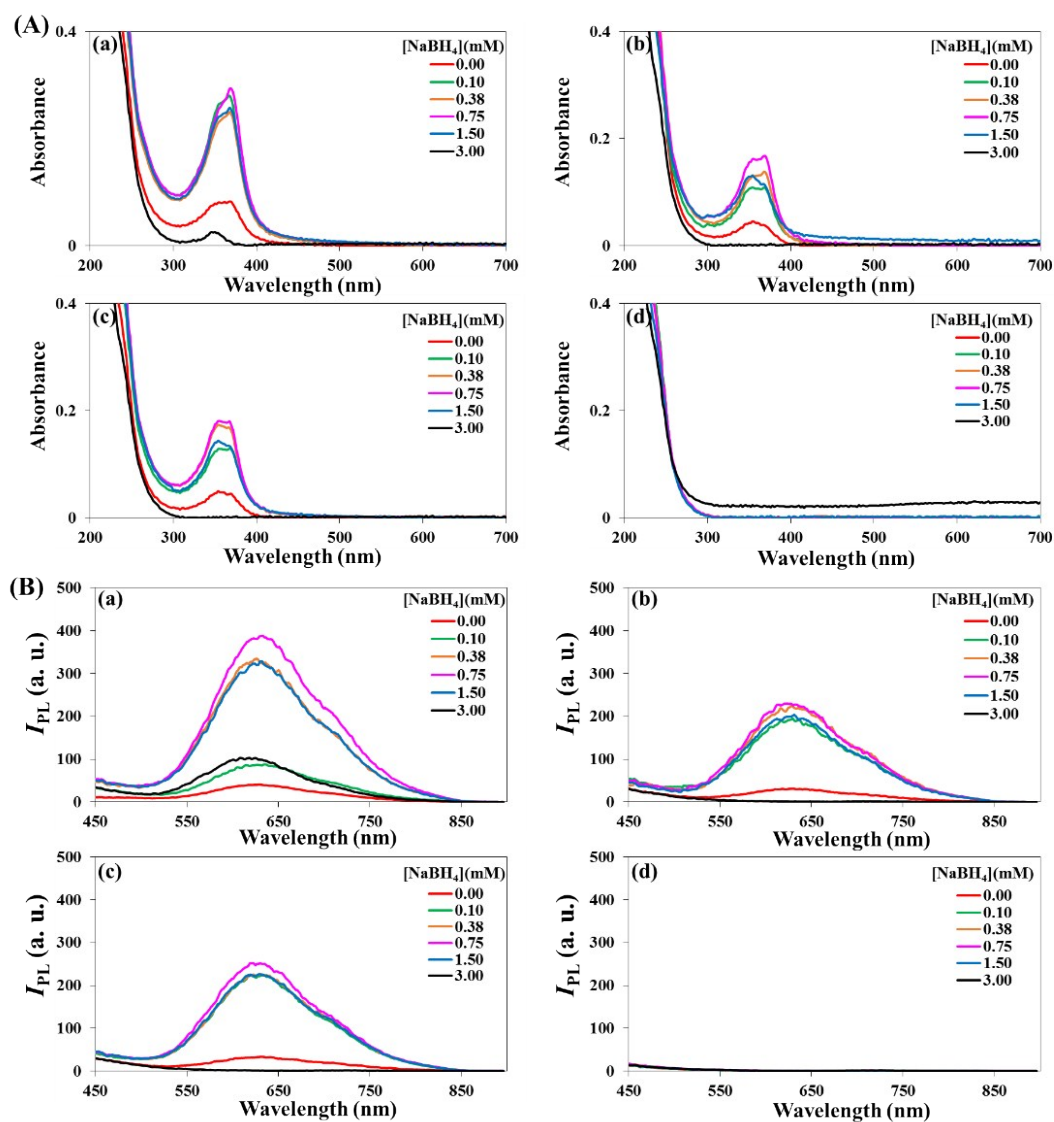


**Fig. S11** (A) UV-Vis absorption and (B) PL spectra excited at 365 nm of (a) Cys-Au NCs<sub>pH3</sub>, (b) Cys-Au NCs<sub>pH5</sub>, (c) Cys-Au NCs<sub>pH7</sub>, and (d)  $-[\text{Cys-Au(I)}]_n\text{-pH9}$  synthesized from the reaction of  $-[\text{Cys-Au(I)}]_n\text{-}$  polymers/supramolecules with  $\text{NaBH}_4$  (0–3.00 mM) for 24 h.

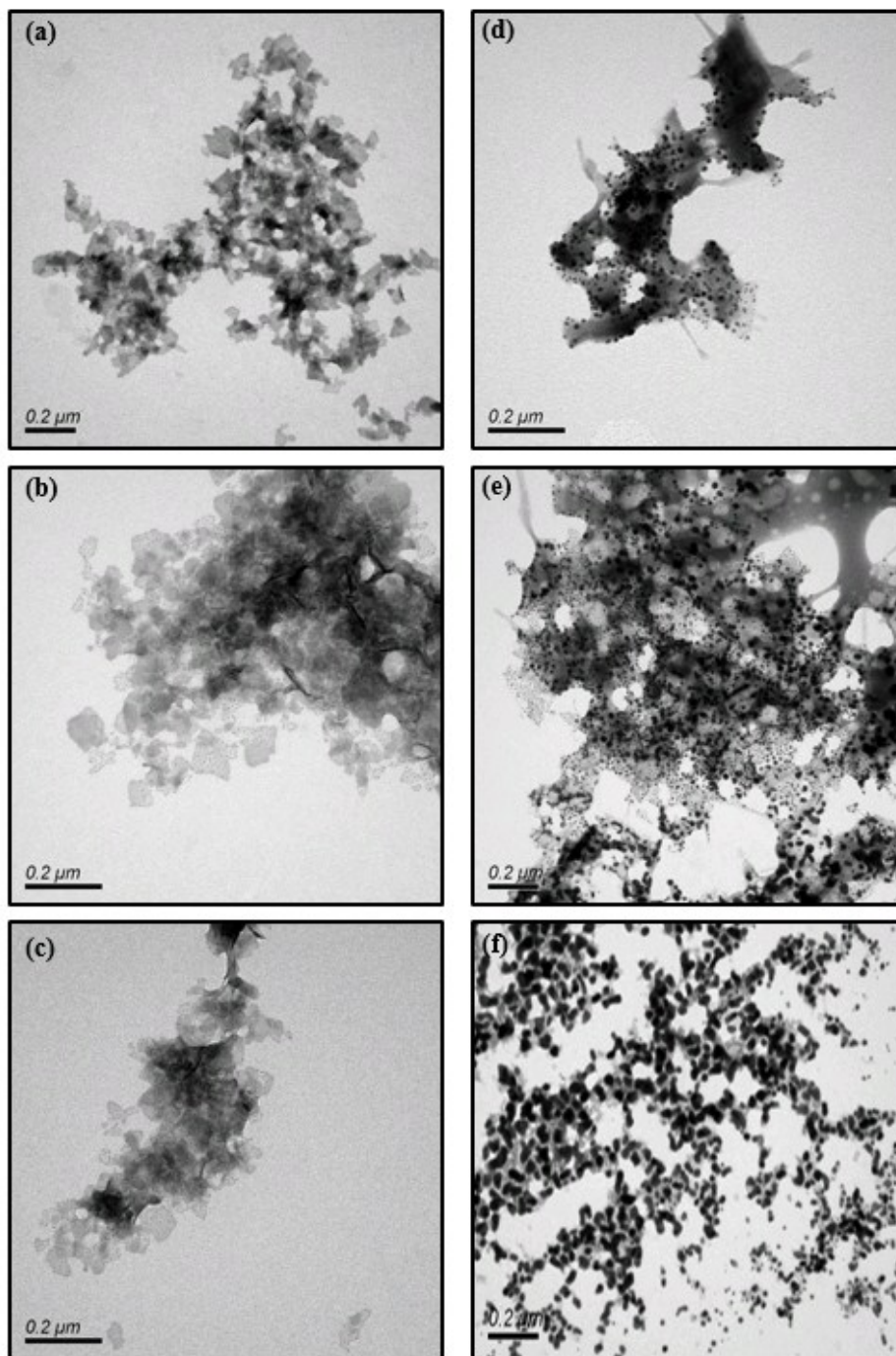


**Fig. S12** TEM images of Cys-Au NCs<sub>pH3</sub>/-[Cys-Au(I)]<sub>n</sub>- supramolecules synthesized from the reactions of -[Cys-Au(I)]<sub>n</sub>- supramolecules for 24 h with NaBH<sub>4</sub> at concentrations of (a) 0 mM, (b) 0.10 mM, (c) 0.38 mM, (d) 0.75 mM, (e) 1.50 mM, and (f) 3.00 mM.

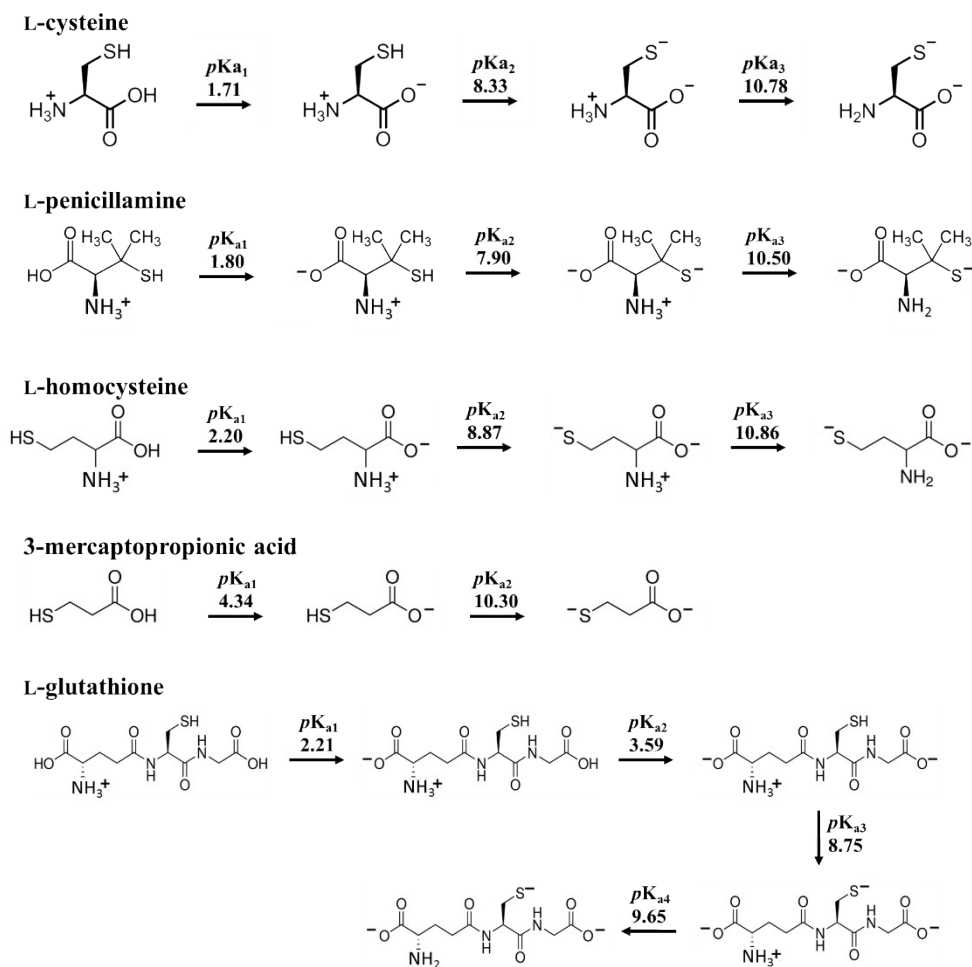


**Fig. S13** Structures and ionizations of L-Cys, L-penicillamine, L-homocysteine, 3-mercaptopropionic acid and reduced L-glutathione.

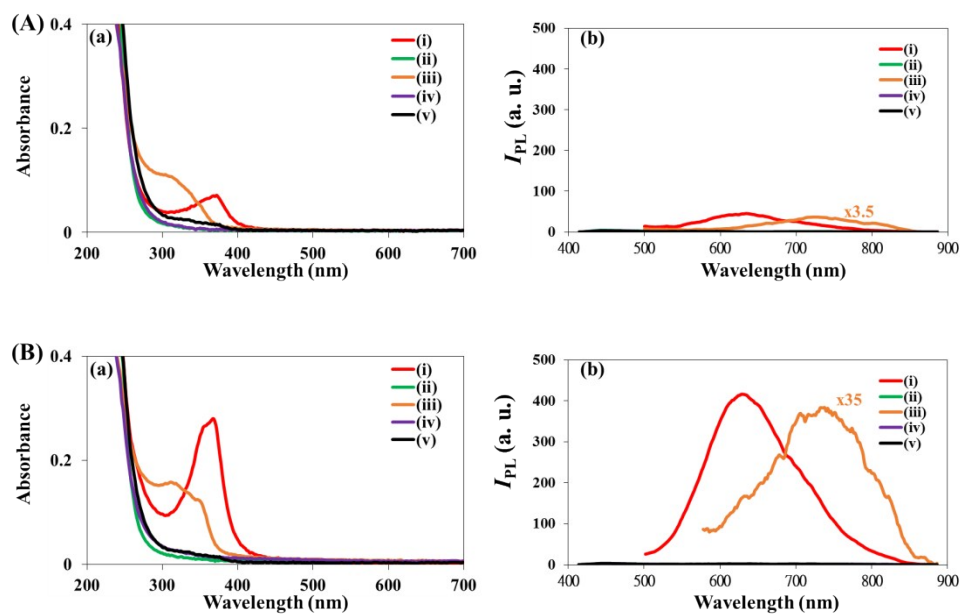


**Fig. S14** (a) UV-Vis absorption spectra and (b) PL spectra excited at 365 nm of (i)  $-\text{[Cys-Au(I)]}_n-$ , (ii)  $-\text{[penicillamine-Au(I)]}_n-$  (iii)  $-\text{[homocysteine-Au(I)]}_n-$ , (iv)  $-\text{[3-mercaptopropionic acid-Au(I)]}_n-$ , and (v)  $-\text{[GSH-Au(I)]}_n-$  synthesized in solutions at pH 3 (A) before and (B) after reaction with NaBH<sub>4</sub> (0.75 mM) for 24 h. .

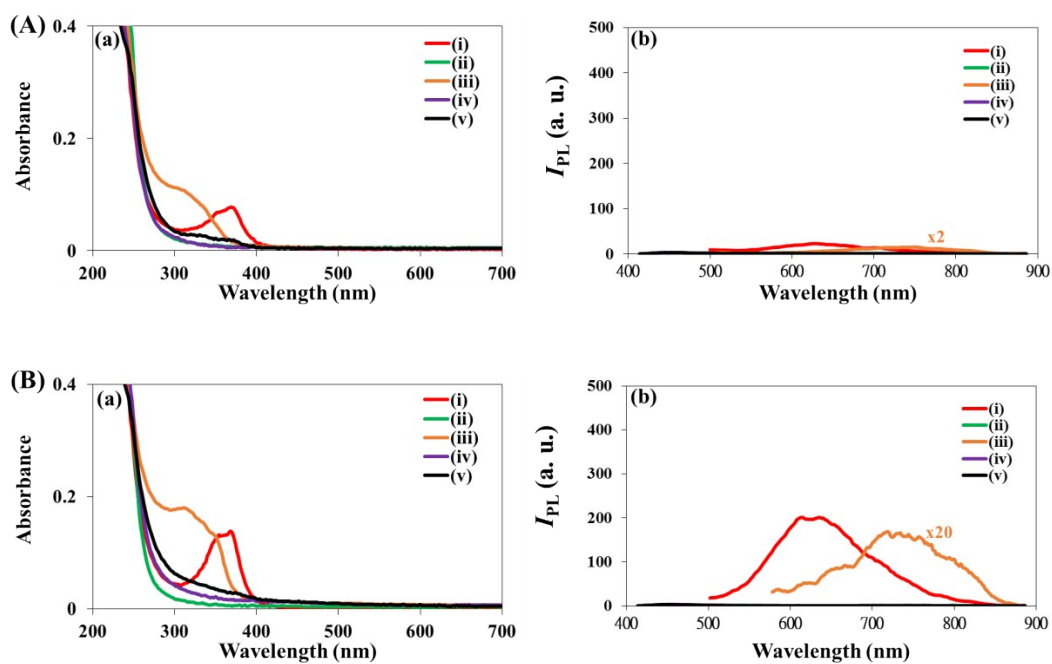


**Fig. S15** (a) UV-Vis absorption spectra and (b) PL spectra excited at 365 nm of (i)  $-\text{[Cys-Au(I)]}_n-$ , (ii)  $-\text{[penicillamine-Au(I)]}_n-$  (iii)  $-\text{[homocysteine-Au(I)]}_n-$ , (iv)  $-\text{[3-mercaptopropionic acid-Au(I)]}_n-$ , and (v)  $-\text{[GSH-Au(I)]}_n-$  synthesized in solutions at pH 5: (A) before and (B) after reaction with NaBH<sub>4</sub> (0.75 mM) for 24 h.

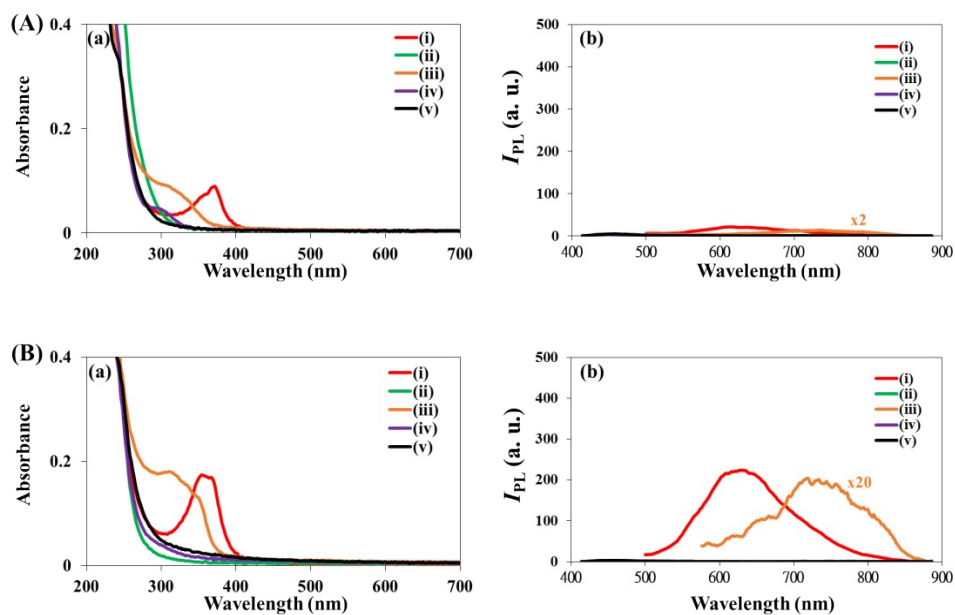


**Fig. S16** (a) UV-Vis absorption spectra and (b) PL spectra excited at 365 nm of (i)  $-\text{[Cys-Au(I)]}_n-$ , (ii)  $-\text{[penicillamine-Au(I)]}_n-$  (iii)  $-\text{[homocysteine-Au(I)]}_n-$ , (iv)  $-\text{[3-mercaptopropionic acid-Au(I)]}_n-$ , and (v)  $-\text{[GSH-Au(I)]}_n-$  synthesized in solutions at pH 7: (A) before and (B) after reaction with NaBH<sub>4</sub> (0.75 mM) for 24 h.

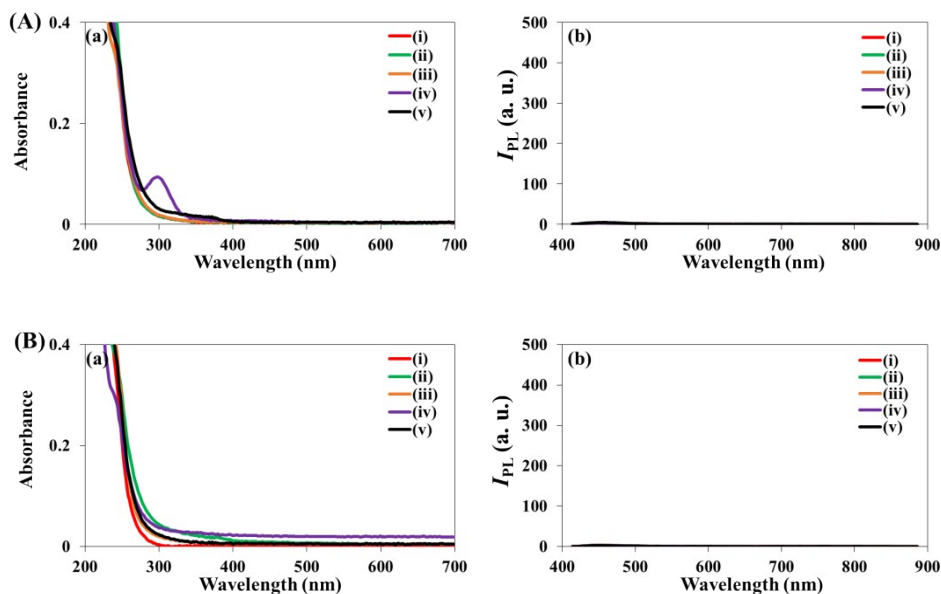


**Fig. S17** (a) UV-Vis absorption spectra and (b) PL spectra excited at 365 nm of (i)  $-\text{[Cys-Au(I)]}_n-$ , (ii)  $-\text{[penicillamine-Au(I)]}_n-$  (iii)  $-\text{[homocysteine-Au(I)]}_n-$ , (iv)  $-\text{[3-mercaptopropionic acid-Au(I)]}_n-$ , and (v)  $-\text{[GSH-Au(I)]}_n-$  synthesized in solutions at pH 9: (A) before and (B) after reaction with NaBH<sub>4</sub> (0.75 mM) for 24 h.